

ANN IN NATURAL GAS TREATMENT PROCESS: CARBON DIOXIDE (CO₂) - ETHANE (C₂H₆) AZEOTROPE SEPARATION

Daniel Chuquin-Vasco^{1, *}, Wendy Dávila³, Nelson Chuquin-Vasco², Juan Chuquin-Vasco²
and Salvador C. Cardona⁴

¹Escuela Superior Politécnica de Chimborazo (ESPOCH), Facultad de Ciencias, Grupo de investigación en seguridad, ambiente e ingeniería (GISAI); daniel.chuquin@espoch.edu.ec (D.CH.V);

²Escuela Superior Politécnica de Chimborazo (ESPOCH), Facultad de Mecánica, Grupo de investigación en seguridad, ambiente e ingeniería (GISAI); nelson.chuquin@espoch.edu.ec (N.CH.V); juan.chuquin@espoch.edu.ec (J.CH.V)

³SOLMA, Servicios de Ingeniería, Quito-Ecuador; wendy.davila@espoch.edu.ec

⁴Instituto de Seguridad Industrial, Radiofísica y Medioambiental (ISIRYM), Universitat Politècnica de València, Plaza Ferrándiz y Carbonell, s/n, E-03801 Alcoy, Spain; scardona@iqn.upv.es

Correspondence: daniel.chuquin@espoch.edu.ec

Abstract: The aim in this study was to develop an artificial neural network (ANN) to forecast the mole fractions of the CO₂- C₂H₆ azeotropic separation during the natural gas treatment process. The ANN was designed with experimental data (150 data pairs) obtained in DWSIM from a previously process described in bibliography. The sample used to train the ANN is structured by three inputs: pressure, temperature and solvent / feed ratio, and six outputs: the mole fractions of distilled CO₂ and residual ethane in the extractive column, the mole fractions of distilled ethane and residual propane in the solvent recovery column and the mole fractions of distilled ethane and residual ethane in the concentrator column. The neural network was designed using 80 hidden neurons in its architecture and the Bayesian regularization algorithm for training (MSE=0.0036 and R=0.9554). The ANN's prediction was validated using statistical parameters (ANOVA and Kruskal Wallis) which indicate that the designed ANN is statistically valid and can be used to predict the mole fractions of the CO₂- C₂H₆ azeotropic separation and can be used in the improvement of the processes of sweetening of natural gas after its demethanization.

Keywords: Azeotrope; Extractive Distillation; Natural Gas; DWSIM; Carbon Dioxide; MATLAB; Artificial Neural Networks (ANN)

1. Introduction

For decades, oil has been the basis of the energy structure worldwide; due to its high level of consumption (90% only in transportation) and extensive development (production of derivative products), it has become the main engine of both developed and developing countries [1]. However, despite the prevalence of oil as the main energy source, natural gas (NG) is currently transforming and changing this trend. NG is known as a mixture of gaseous hydrocarbons that is frequently found in fossil deposits in various forms, such as: non-associated (alone), dissolved or

associated (accompanying oil) and in coal deposits [2], and constitutes the third energy source worldwide after oil and coal.

The composition of NG can change according to the type of reservoir, depth, location and geological conditions. However, for the gas to be used commercially or industrially, it must undergo a conditioning pretreatment, which is mainly based on the removal of water content and acid gases characteristics of its composition [3]. NG treatment generally involves four stages: sweetening, dehydration, oil removal and liquefaction [4].

There are several methods for NG sweetening: chemical absorption with amines, physical absorption, membrane permeation, and low-temperature distillation [5]. The low-temperature extractive distillation process (conventional process) separates CO₂ from hydrocarbons through a sequence of two distillation columns and is one of the most widely used because it minimizes operational and safety problems [6]. However, despite its widespread industrial use and its major benefits, its high energy demand commonly accounts for more than 50% of plant operating costs [6,7].

In this regard, several studies to optimize the CO₂-C₂H₆ separation process stand out. For example, Torres et al., [8] analyzed by simulation the effect of different fractions of liquefied hydrocarbons as a drag agent, the thermodynamic efficiency and the generation of greenhouse gases in conventional process to remove CO₂. This alternative presented better overall performances compared to the conventional chemical absorption system. Lastari et al. [9] analyzed the effect of the solvent/feed composition and the location of the feed trays on the total energy requirement, establishing that the optimum solvent/feed ratio is in the range of 1.053 - 1.064 for the treatment of the mixture (CO₂- C₂H₆) and that the stage where the feed and solvent enter has significant effects on the total energy demand of the column.

On the other hand, Tavan et al. [10] established through simulation in ASPEN HYSYS that there is a significant reduction in operating costs (total energy demand) using reactive absorption (RA) configurations making use of diethylamine as solvent, compared to conventional extractive processes. They then proposed, by means of rigorous simulation methods, an extractive dividing-wall column (EDWC) taking into account environmental (CO₂ emission) and energy parameters and confirmed that this technology reduces the total energy demand by approximately 51.6% [11]. In addition, they proposed the feed-splitting technique, to separate the feed prior to entering the heat exchanger, in order to maintain a fraction of the feed at its original temperature. By means of this technique, the energy reduction in contrast to the conventional process is 56% [12]. With the aforementioned, EDWC is one of the most efficient and operative techniques, which allows an approximate saving of 17% in total annual costs [7]. It is important to mention hybrid technologies to minimize energy costs in distillation processes, this technology reports the advantages of a profitable process units [13–15].

Ebrahimzadeh et al., [5] suggest a three-column extractive distillation configuration for CO₂-C₂H₆ separation (ASPEN PLUS simulation). The process described leads to a 10% reduction in annual cost without compromising the desired purification, and also significantly minimizes the energy required for liquefaction.

1.1. ANN as a prediction tool in chemical processes

ANNs are able of solving linear and nonlinear multivariate regression problems, hence permitting the study of the relationship between the input and output variables of the method employing a constrained number of test runs. In addition, ANNs can be effortlessly created by applying an appropriate plan of tests [16,17].

ANN models have been applied in several chemical processes, such as nonlinear multi-variable predictive controllers for distillation columns, where the controller uses an on-line optimization routine, which determines the future control variables that minimize the deviations between the predicted control variables and their set points [18]. Zamproga et al. [19] designed a virtual sensor (recurrent ANN) that estimates product compositions, using measurements of secondary parameters such as temperature and molar flow, in a batch distillation column of intermediate vessels. The work showed that the estimated compositions match the actual values. Li et al. [20] combined ANNs with genetic algorithms (GA) to model the azeotropic distillation system of isopropanol-water mixture with complex mechanisms and optimize the energy.

Liau et al. [21] designed an ANN capable of predicting the quality of the crude oil as a function of the input parameters, thus optimizing and maximizing the production rate and the process. The developed system provides the optimal operating conditions of the fractionation unit considering the operating variables. Fernandez et al. [22] built an identification and control tool for a laboratory-scale distillation column based on neural networks using LABVIEW. They demonstrated that ANNs are a potential tool for their functionality when interacting with instruments, sensors and actuators.

Motlaghi et al. [23] created an ANN model of a crude oil distillation systems (CDU), to forecast the unspecified values of the desired product flow and temperature at the specified characteristics of the input feed, being able to minimizing the model output error and maximizing the required oil generation rate with respect to control parameter values (product quality).

On the other hand, Vafae et al. [24] used a multilayer perceptron (MLP) network as a new and effective method to simulate recoveries from 16 oil data sets using as input variables: API degrees, viscosity, characterization factor and steam distillation factor, to predict distillation performance. This study showed that MLP is more effective than the EOS equation of state method and Holland - Welch correlation.

In addition, Ochoa et al. [25] suggest a methodology to optimize heat-integrated in CDU, which considers an ANN model to represent the distillation column. The ANN is incorporated into the process in an optimization system to efficiently decide the working conditions that progress the overall economy of the process.

Leng et al. [26] used a back propagation ANN to build a model between the physical properties and Terahertz spectra -THz- (technique used to realize the identification and determination of the principal gas components distilled from oil shale) with the input of THz-FDS over the range from 0.2 to 1.5 THz to quantitatively characterize the component and total pressure of the distillation process. The results indicate that the THz (Terahertz) technique combined with ANN is an effective tool for gas detection and can be used in industrial unconventional gas plants.

Osuolale and Zhang [27] presented a neural network-based strategy to model and optimize energy efficiency in distillation columns. They used ASPEN HYSYS for distillation system simulation and ANN models to obtain optimal operating conditions that can maximize energy efficiency, quality, and product yield. The application of the proposed methodology improved 32.4% of exergetic efficiency.

There are several investigations that employ neural network models applied to chemical processes, however, the alternative processes of extractive distillation and separation of azeotropes have not been exploited within the ANN area. The advantage over simulation is that ANN is able to learn directly from a process and give shorter response times, allowing systems to be modeled in a more complex and realistic manner [28,29]. Other advantages are its simplicity, versatility, accurate approximation of complex nonlinear processes and "black box" approach; it does not require detailed knowledge of the system being analyzed[30,31].

In the present work we propose to generate an ANN, from Chemical Process Simulator open source (DWSIM), of the process proposed in [5] to predict the mole fractions of the main components obtained in the extractive distillation, both in the distillate and in the residues of each extractive column, as a function of the operating conditions of the process. In the future, ANN can be incorporated into industrial plants for prediction, optimization, and continuous improvement of processes.

2. Materials and Methods

2.1. Process Description

Figure 1 illustrates the alternative extractive distillation process for the separation of azeotrope CO₂-C₂H₆, adapted from [5]. The process is composed of three columns: C1 - CO₂ extractive column, C2 - solvent recovery column and C3 - concentrator column.

Column (C1) receives a free methane stream from a natural gas demethanizer (not considered in the process) containing CO₂, C₂H₆ and hydrocarbons, which is mixed with the recirculation from the distillate of column (C3) containing CO₂ and C₂H₆. In addition, the bottom product (hydrocarbons) from the column (C2) also enters in column (C1).

During the process, in C1 the head product is not entirely CO₂ and the bottom product contains 10% CO₂ together with C₂H₆ and heavy hydrocarbons.. In C2, the high purity solvent from the bottom stream of the first column is recovered at the base of the second column and the distillate from this column is fed to the third column (C3), which produces C₂H₆ (bottom) and azeotropic mixture (distillate).

Table 1 summarizes the composition of the feed entering the extractive column C1. While Tables 2-4 detail the operating conditions of the extractive, solvent recovery and concentrator columns, respectively. Unlike the conventional process, the distillate from the extractive column remains in a liquid state and does not require a liquefaction process, thus minimizing the total energy demand. The heavy hydrocarbons leaving the solvent recovery column as a bottom product are divided into NGL product and solvent, which is recycled back to the extractive column (recirculation 1). In C3 the bottom product is C₂H₆ with high purity (99.7 mole %), while distillate is CO₂-C₂H₆ mixture (1.35 kmol/s, 46.2 mole % CO₂). After heat recovery, it is recycled to C1 (recirculation 2 – Feed Stage = 5).

The thermal power source used for all heat exchangers is saturated steam at 6.9x10⁵ Pa. In addition, as opposed to the conventional design using a total condenser, partial condensers are used in the solvent recovery column and concentrator.

Table 1. Feed Conditions to C1

Parameter	Quantity	Unit
Pressure	2.43e6	Pa (abs)
Temperature	320.15	K
Feed base (molar flow)	4	kmol/s
Initial composition of CO ₂ *	0.3225	-
Initial composition of C ₂ H ₆ *	0.4623	-
Initial composition of propane C ₃ *	0.0753	-
Initial composition of isobutane i-C ₄ *	0.0753	-
Initial composition of butane n-C ₄ *	0.0323	-
Initial composition of isopentane i-C ₅ *	0.0215	-
Initial composition of pentane n-C ₅ *	0.0108	-

Source: Ebrahimzadeh et al., [5]

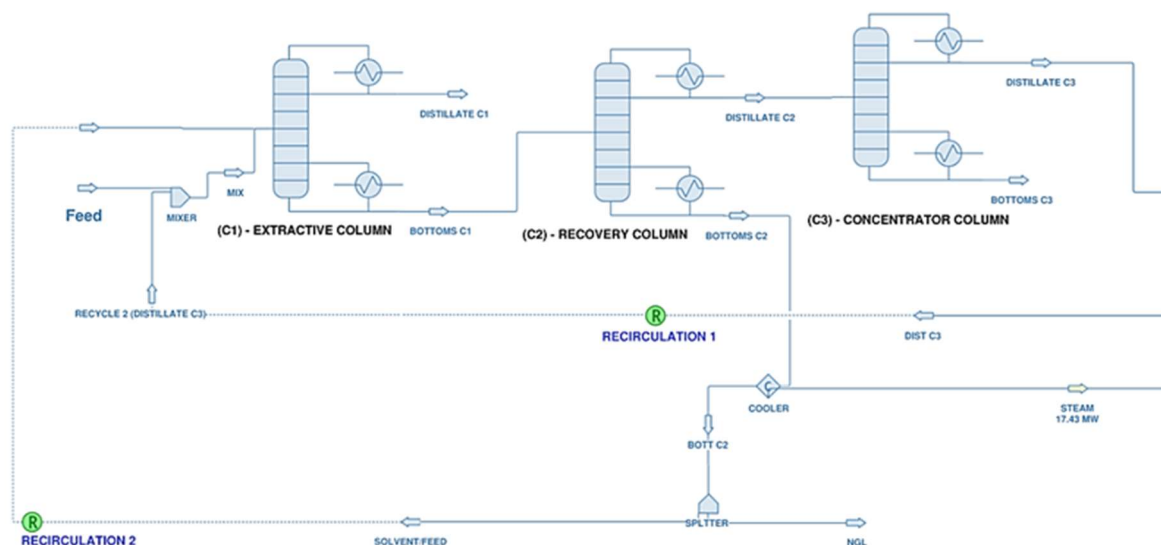


Figure 1. Simulation of the alternative distillation system to separate CO₂- C₂H₆ azeotropes in DWSIM

Table 2. Extractive column operating conditions

Parameter	Quantity	Unit
Pressure	2.3e6	Pa (abs)
# Column stages*	39	-
# Feed stage*	36	-
# Solvent inlet stage*	5	-
Solvent/feed ratio	0.6	-
Reflux ratio (RR)	4.61	-
Solvent molar flow (recycle stream from C2)	2.4	kmol/s
Feed molar flow	4	kmol/s
Molar flow of recycle stream from C3	1.35	kmol/s
Condenser duty	87.86	MW
Reboiler duty	15.12	MW

Source: Ebrahimzadeh et al., [5]

Table 3. Solvent recovery column operating conditions

Parameter	Quantity	Unit
Pressure	2.3e6	Pa (abs)
# Column stages*	37	-
# Feed stage*	15	-
Reflux ratio (RR)	1.08	-

Condenser duty	32.1	MW
Reboiler duty	92.6	MW

* Numbered from the top of the distillation tower.

Source: Ebrahimzadeh et al., [5]

Table 4. Concentrator column operating conditions

Parameter	Quantity	Unit
Pressure	2.3e6	Pa (abs)
# Column stages*	43	-
# Feed stage*	10	-
Reflux ratio (RR)	2.9	-
Condenser duty	37.1	MW
Reboiler duty	20.9	MW

Source: Ebrahimzadeh et al., [5]

2.2. Metodology

Fig. 5 details the methodological procedure for the development of the ANN. As a first point, the simulation and validation of the process detailed in Fig. 1 is carried out based on the operating conditions of Tables 1-5. Subsequently, the ANN is designed and validated considering the inputs and outputs described in Figs. 3-5 and the constraints defined by the simulation. Finally, the functionality and predictive capacity of the ANN is evaluated through a graphic and statistical analysis.

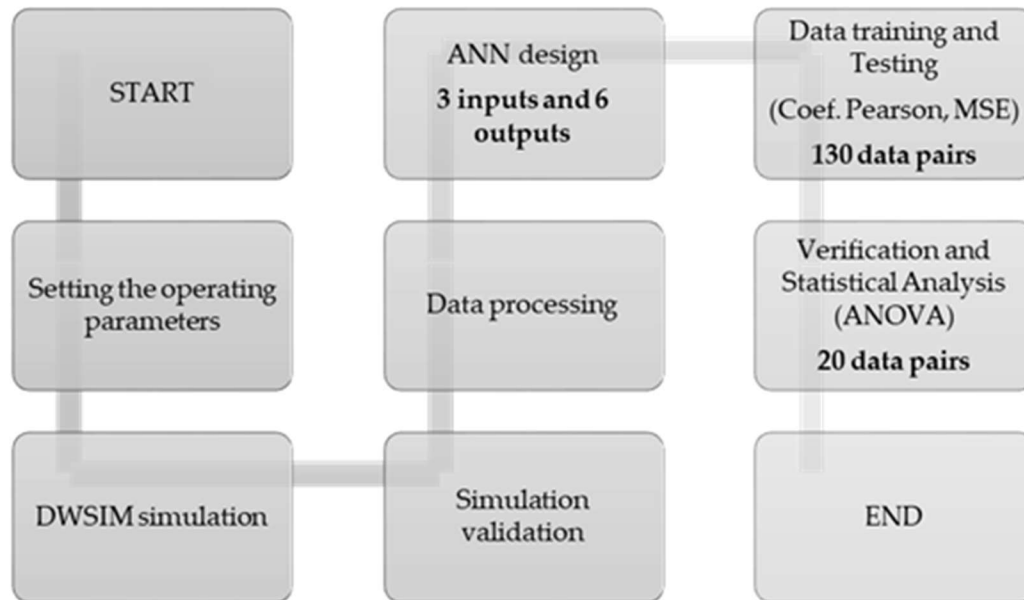


Figure 2. Methodological scheme of the designed ANN

2.3. DWSIM simulation

DWSIM (open-source chemical process simulator) is available for Windows, Linux, Android, macOS, and iOS and allows engineers to model process plants by using rigorous thermodynamic and unit operations [32].

The distillation towers used for the simulation in Fig. 1 correspond to the "Chem-Sep Column" model. All flow streams operate with the Peng-Robinson (PR) properties package, while for the distillation towers the EOS / Predictive PR 78 thermodynamic models are adapted, which is one of the most widely used packages in hydrocarbon modeling and in principle are able to estimate the phase equilibrium and other thermodynamic properties of a wide assortment of frameworks [33–35]. The conditions established in Tables 2-4 correspond to the operating conditions under which the process simulation was carried out. It is important to note that the ChemSep columns require the specification of only two operating parameters in addition to the pressure value.

The mathematical method, we used to find the convergence of the simulation process was Newton's Method for which a maximum of 100 iterations was established.

2.4. Design and training of the ANN

The ANN design (Figure 3) is based on three input parameters: pressure (C1, C2 and C3), temperature (inlet temperature to column C1) and solvent/feed ratio to column C1. These input variables were chosen because of the importance they represent in the quality of the final products and in optimization processes [9,10,36–38]. While six output parameters were considered: mole fractions of CO₂ distillate and C₂H₆ bottom in C1, C₂H₆ distillate and C₃ bottom in (C2), and C₂H₆ both distillate and bottom in (C3).

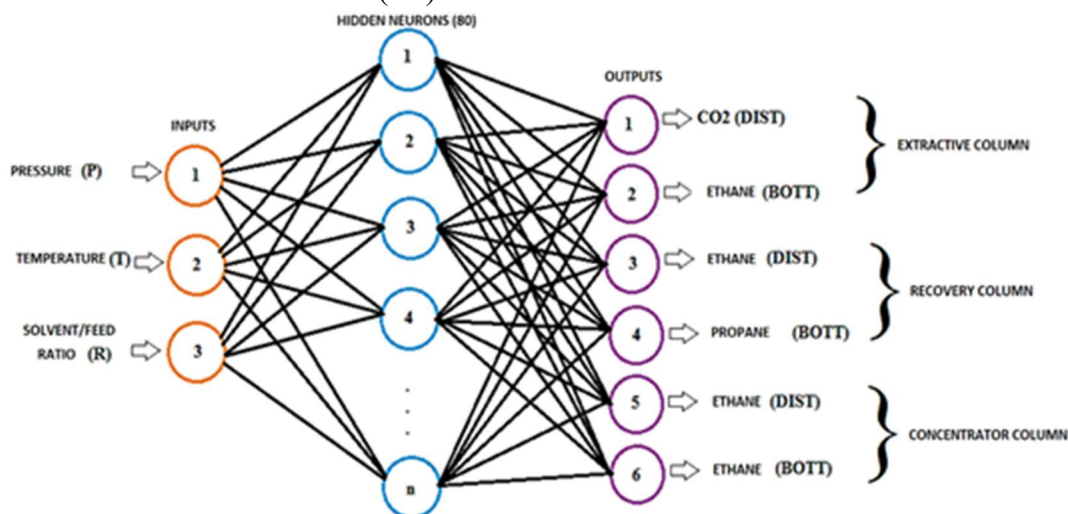


Figure 3. Schematic of the designed ANN

Based on the guidelines of Chen et al., [39], for network learning and training 70% of the total data pairs (90 data sets) were used, while 30% (40 data sets) were utilized to perform a testing to assess its level of learning. Figures 4 and 5 describe the inputs and outputs used in the ANN designed (Appendix A).

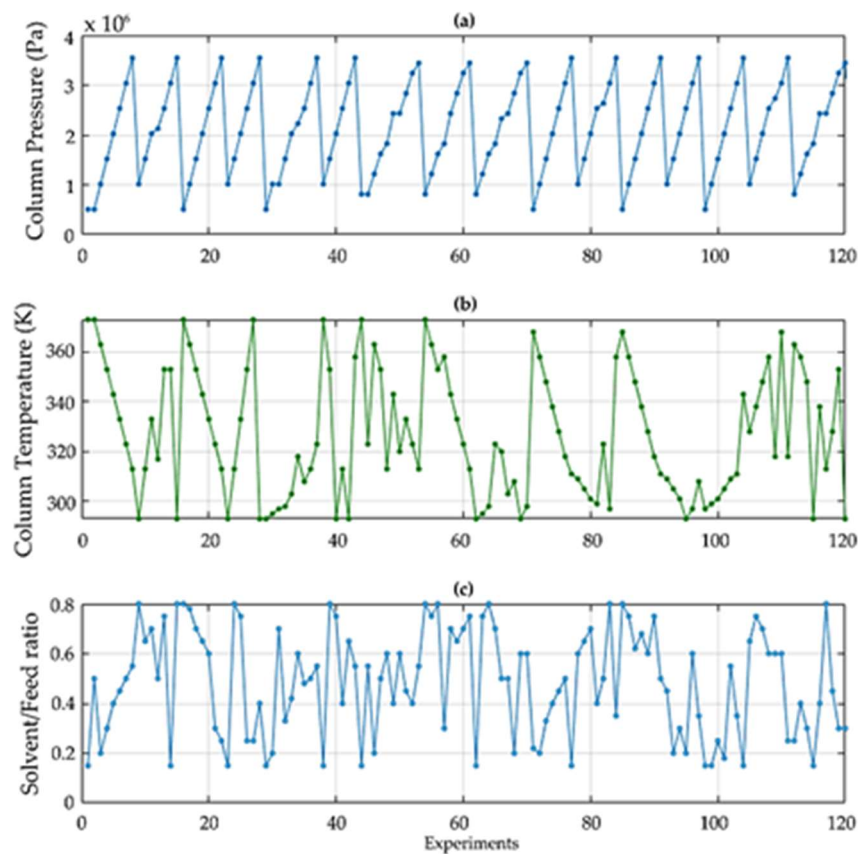


Figure 4. Inputs: (a) Columns pressure (Pa); (b) Columns temperature (K); (c) Solvent/feed ratio
The ANN training adjusts the weights of the connections between neurons for the ANN to make adequate predictions regarding the targeted output data. Validation measures the ANN's prediction errors to assess its performance. Testing process evaluates the prediction of ANN using pairs of data that were not used in the training process [40].

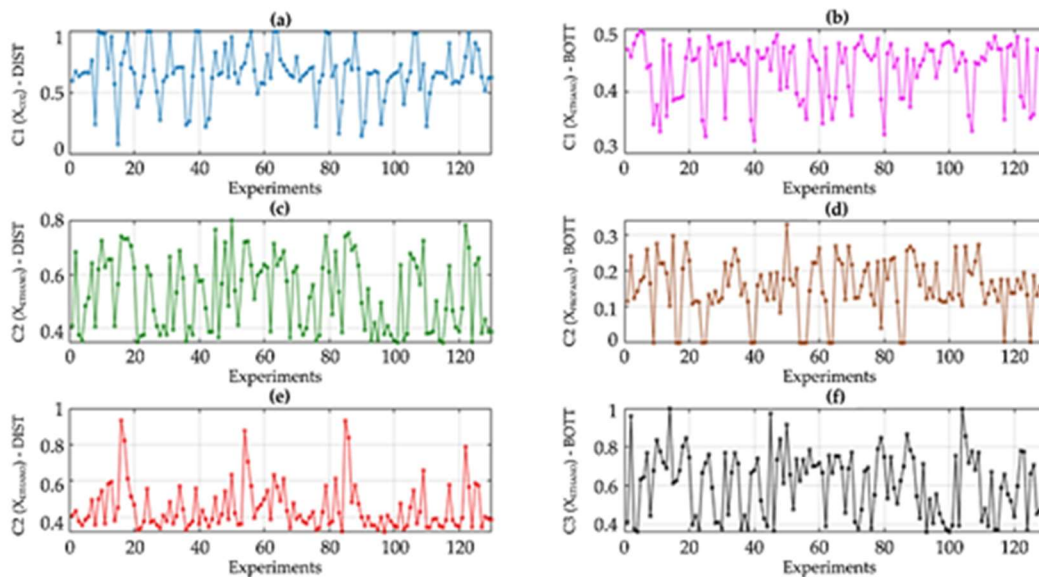


Figure 5. Outputs: (a) Mole fraction of CO₂ distillate in C1; (b) Mole fraction of C₂H₆ bottom in C1; (c) Mole fraction of C₂H₆ distillate in C2; (d) Mole fraction of C₃ bottom in C2; (e) Mole fraction of C₂H₆ distillate in C3; (F) Mole fraction of C₂H₆ bottom in C3.

The specific bibliography in ANN, suggests at least 50 points to predict quantities with regression algorithms [41–43]. In this respect, 130 pairs of data (with 3 inputs and 6 outputs) was generated, coming from the random variation of the operating parameters and/or performances selected for the study. Table 5 shows the range of variation of the inputs, that were chosen based on typical and extremes ranges of operation [9,10,36–38]. To ANN validation, we used the following performance indicators: mean square error (MSE) and regression coefficient (R) by means of Eq. (1) and Eq. (2) and additionally an ANOVA. In addition, the ANN performance was optimized through a trial-and-error procedure in order to minimize the MSE and maximize the correlation coefficients in the training, validation and testing stages.

$$MSE = \frac{1}{n} \sum_{t=1}^n (y - y')^2 \quad (1)$$

$$R = \frac{n \sum_{i=1}^n (y' y) - [\sum_{i=1}^n y'] [\sum_{i=1}^n y]}{\sqrt{[n \sum_{i=1}^n y^2 - [\sum_{i=1}^n y]^2] [n \sum_{i=1}^n y'^2 - [\sum_{i=1}^n y']^2]}} \quad (2)$$

Where: n is the number of observations; y are the actual results (simulation out-puts); y' are the predicted targets (ANN outputs).

Parameter	Pressure (Pa) C1, C2, C3	Temperature (K) inlet stream to C1	solvent/feed ratio (-) regulated in the splitter
*Range	506625 – 3.54e6	2.93.15 – 373.15	0.15 – 0.8

* Less or greater than the established ranges, the simulation does not run.

3. Results and discussion

This section presents the analysis and discussion of the process simulation and the design, training and validation of the ANN.

3.1. Simulation validation

The validation of the simulation process in DWSIM was carried out with the comparison of the study developed in ASPEN PLUS by Ebrahimzadeh et al. [5]. Table 6 summarizes the percentage errors of the mole fractions of interest in their respective distillation columns, which do not exceed 3%. This percentage of error is justified by the presence of very small traces of other constituents in the distillate and the bottom currents, which are considered negligible.

3.2. ANN topology

This section describes the design and structuring of the ANN by analyzing the correlation coefficient (R) and the mean square error (MSE).

3.2.1. Selection of ANN Training Algorithm

For the design and structure of the ANN, three training algorithms were used: Levenberg - Marquardt (LM), Bayesian regularization (BR) and scaled conjugate gradient backpropagation (SCG). According to specialized bibliography, these algorithms minimize the MSE to a greater extent compared to other algorithms available in the literature [44–46]. As in other prediction studies [47,48], the R and MSE values (Table 7) were evaluated for the 3 algorithms studied by varying the number of neurons in the hidden layer.

Table 6. Simulation validation (mole fraction)

Column	Parameter	Aspen Plus [Ebrahimzadeh et al., 2016]	DWSIM	Error (%)
Extractive (C1)	CO ₂ distillate	0.956	0.953	0.24
	C ₂ H ₆ bottom	0.396	0.406	2.60
Recovery (C2)	C ₂ H ₆ distillate	0.799	0.801	0.29
	C ₃ bottom	0.337	0.328	2.59
Concentrator (C3)	C ₂ H ₆ distillate	0.538	0.554	2.98
	C ₂ H ₆ bottom	0.997	0.975	2.25

Table 7. Pearson's correlation coefficient (R) and root mean square error (RMSE) values for trial and error using Levenberg–Marquardt (LM), Bayesian regularization (BR) and scaled conjugate gradient backpropagation (SCG) algorithms.

# hidden neurons	LM		BR		SCG	
	R Global	MSE	R Global	MSE	R Global	MSE
20	0.930	0.0074	0.959	0.00187	0.901	0.0129
40	0.926	0.0076	0.948	0.00181	0.899	0.0095
60	0.916	0.0065	0.873	5.81 E-07	0.895	0.0072
80	0.889	0.0096	0.955	0.00160	0.864	0.0078
100	0.961	0.0068	0.901	1.29 E-11	0.843	0.0033

After the training process, the results detailed in Table 8 conclude that the most suitable and robust model to predict the output targets is BR (MSE min = 1.29E-11, R max = 0.955). The advantage

of a BR algorithm is its ability to predict complex relationships and its ability to make decisions less biased [44,49,50].

The computational cost of the BR algorithm is higher, compared to other training algorithms, however, it gives rise to good generalizations for difficult, small or noisy data sets. Furthermore, it shows a better performance of the predictive capacity in contrast to the Levenberg-Marquardt algorithm. The advantage lies in its ability to handle potentially complex relationships, which means that it can be used in quantitative studies to provide a robust model[44].

3.2.2. Selection of the number of neurons in the hidden layer

The determination to the optimal neuron's number it's useful to conduct trials in determining required local minimum in the error surface, and oscillations in R [2].

According to the analysis in Table 8, when 20 and 80 neurons are used in the hidden layer, the best R values are obtained in the testing and global phase. For 20 neurons the R value in testing is 0.846 and for 80 neurons 0.841, while the MSE values for 20 and 80 neurons are: 0.0018765 and 0.0001609. The results would indicate that the optimal number of neurons is 80. As seen in Table 9, the lowest percentage error (< 9 %) occurs when 80 neurons are used in the hidden layer.

Table 8. R and MSE values for determining the optimal number of neurons in the hidden layer

# hidden neurons	R Training	R Testing	R Global	MSE
20	0.979	0.846	0.959	0.00187
40	0.979	0.802	0.948	0.00181
60	0.999	0.640	0.873	5.81 E-07
80	0.978	0.841	0.955	0.000160
100	0.999	0.625	0.901	1.29 E-11

Table 9. Percentage error (%E) values for determining the optimal number of neurons in the hidden layer

# hidden neurons	%E CO ₂ Distillate C1	%E C ₂ H ₆ Bottoms C1	%E C ₂ H ₆ Distillate C2	%E C ₃ Bottoms C2	%E C ₂ H ₆ Distillate C3	%E C ₂ H ₆ Bottoms C3
20	66.75	12.15	24.63	16.72	42.95	39.01
40	54.63	11.26	29.05	39.84	54.56	27.58
60	77.54	11.29	28.07	41.68	53.86	35.70
80	8.03	2.54	4.18	8.53	5.90	6.09
100	62.90	13.27	39.75	26.46	85.03	50.69

The ANN (perceptron type) was designed with MATLAB NNTOOL version R2018a and from the analysis developed, it is defined that the structure of the ANN is composed of: three (3) input neurons, a hidden layer with 80 neurons and six (6) output neurons. According to the study developed by Abiodun et al.,[51] a hidden layer may be sufficient for prediction in most ANN applications.

3.2.3. ANN training and testing

Table 10 shows the MSE values for the training phase and testing phase of the ANN. For the validation phase there are no results. This is justified because ANNs using the BR algorithm are more robust models and can reduce or eliminate the need for validating, taking advantage of these data during training. The MSE values for the training and testing phase are: 0.0036 and 0.0222 respectively, indicating that the ANN performs adequately and that the predictions are made with sufficient accuracy. Figure 6 shows the evolution of the mean square error (MSE) during the training phase, with a final MSE of 0.0036. The MSE performance function for the training data (train) is very close to zero, indicating that the predictive capability of the network is very good.

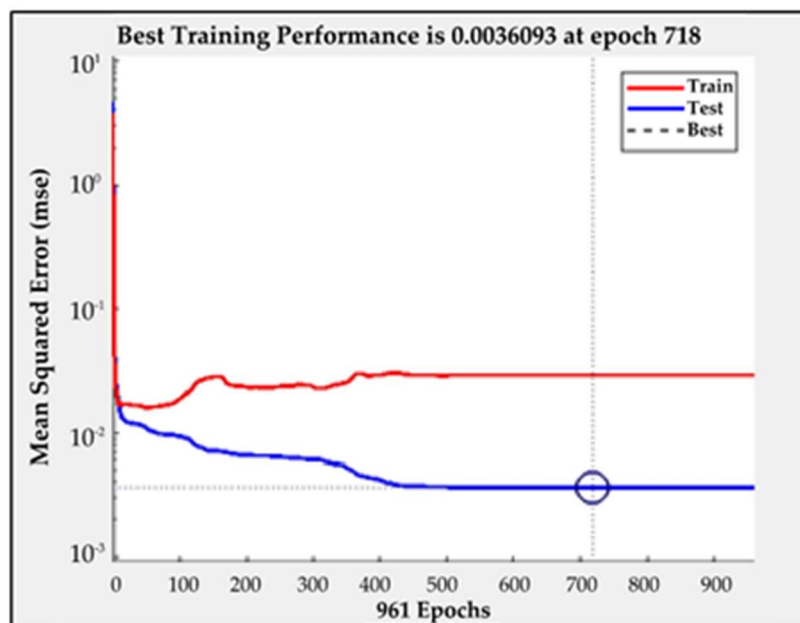


Figure 6. ANN training performance (MSE)

On the other hand, as seen in Fig.7, there is a moderate dispersion between the outputs and targets of the ANN in both the training and test phases. However, the R values for the training and testing phase are 0.98 and 0.84 respectively, and the overall R value of 0.96 which indicates that the outputs and targets have an acceptable correlation. The closer the R value is to 1, the better the performance of the ANN. To validate the ANN, the decision was made that the R value should be in the range of 0.95 to 1 and the MSE lower than 0.025.

Table 10. Mean square error of ANN designed

PHASE	MSE
trainPerformance (training)	0.0036
testPerformance (testing)	0.0222

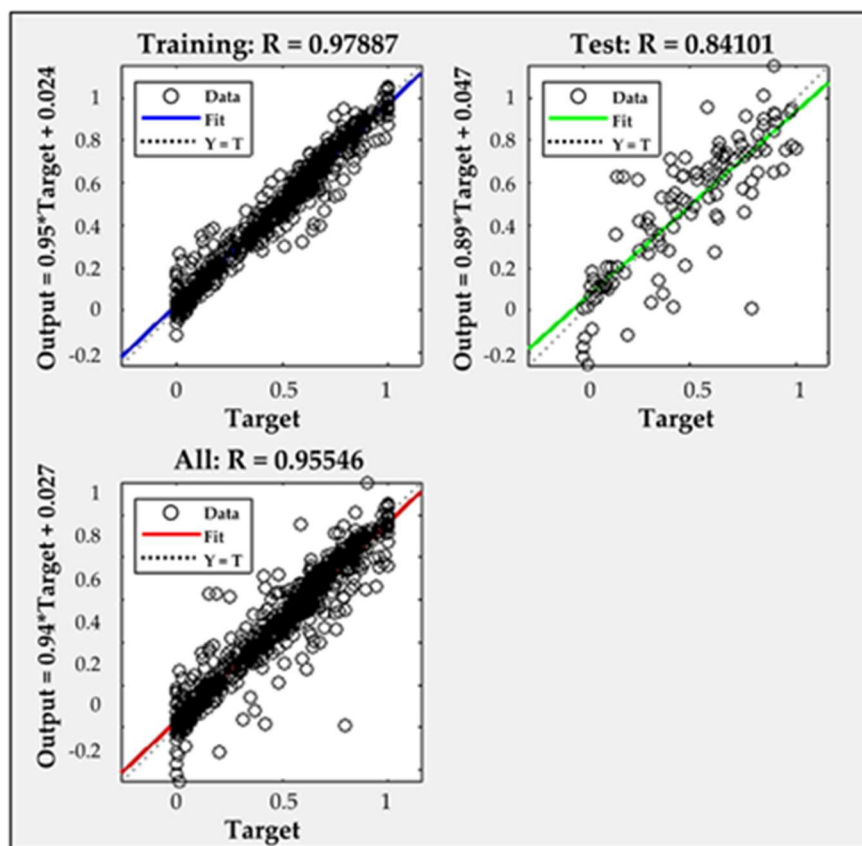


Figure 7. Regression coefficient R for ANN training and testing

3.3. Model prediction of CO₂, C₂H₆ and C₃ mole fractions in the extractive, solvent recovery and concentrator columns.

Figures 8 -9, 10-11 and 12-13 show the overlap between the experimental values (obtained by simulation) and the predictions (obtained by ANN) in the extractive column, solvent recovery and concentrator, respectively. It can be seen that the comparisons obtained in the three columns are relatively equal. The developed model clearly approximates the observational data (simulation) proving in this way that the ANN constitutes a robust and adequate model for the prediction of C₂H₆ and CO₂ concentrations and that it can be applied in CO₂- C₂H₆ azeotrope separation process in enhanced oil recovery processes.

Based on the analysis of Figures 8-13, the average percent error (%E) of the predictions are: 5.036% (CO₂ in the distillate) and 2.55 % (C₂H₆ in the residue) in the extractive column (C1); 4.19% (C₂H₆ in the distillate) and 4.18% (C₃ in the residue) in the solvent recovery column (C2); 5.91% (C₂H₆ in the distillate) and 6.09% (C₂H₆ in the residue) in the concentrator column (C3).

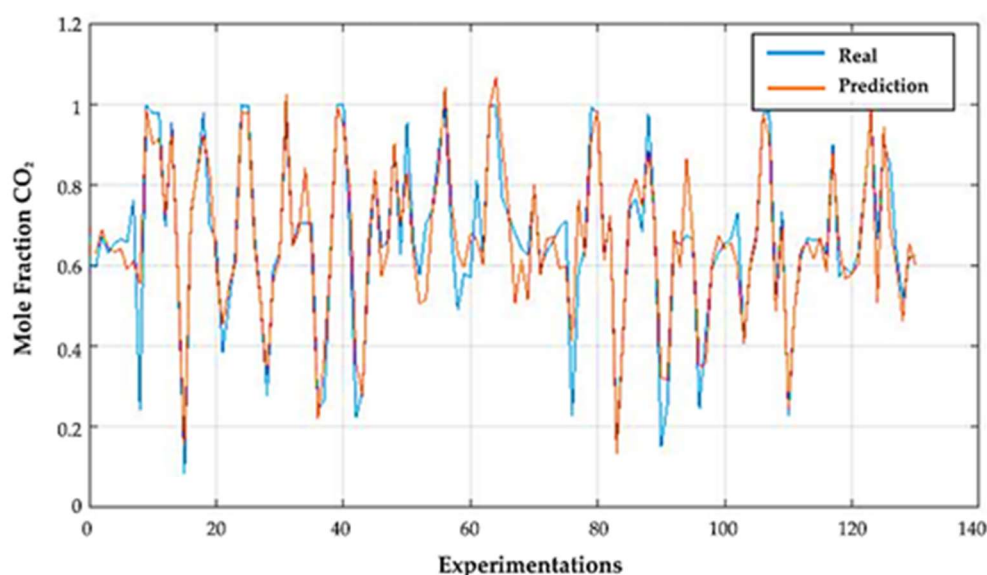


Figure 8. Comparison of DWSIM (real) and ANN (predicted) results in extractive column distillate (CO_2 mole fraction)

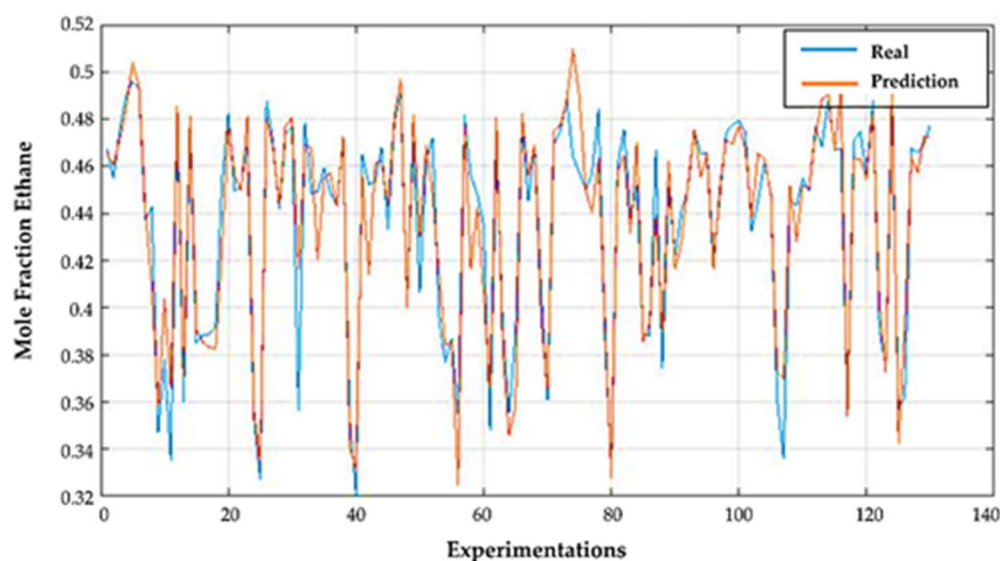


Figure 9. Comparison of DWSIM (real) and ANN (predicted) results on the extractive column bottoms (C_2H_6 mole fraction)

3.4. ANN model verification

The ANN predictive capacity of the concentration of CO_2 , C_2H_6 and C_3 in the ex-tractive, solvent recovery and concentrator column was tested with a set of 20 random input data (P, T and solvent / feed ratio) unknown by the ANN. The results show an overlap between the experimental data and the predictions. This indicates that ANN has a good predictive capacity of the mole fractions of distillates and residues of the distillation columns (Fig.14).

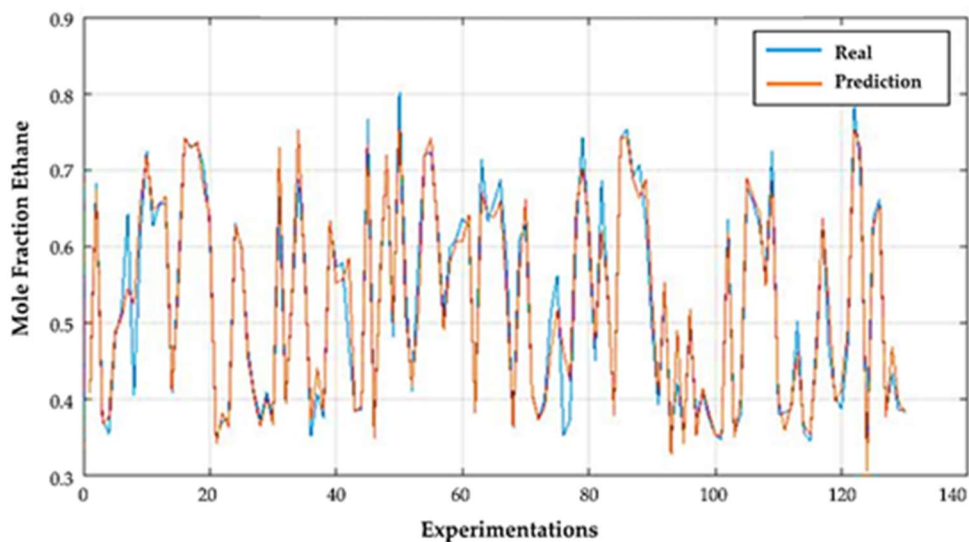


Figure 10. Comparison of DWSIM (real) and ANN (prediction) results in solvent recovery column distillate (C2H6 mole fraction)

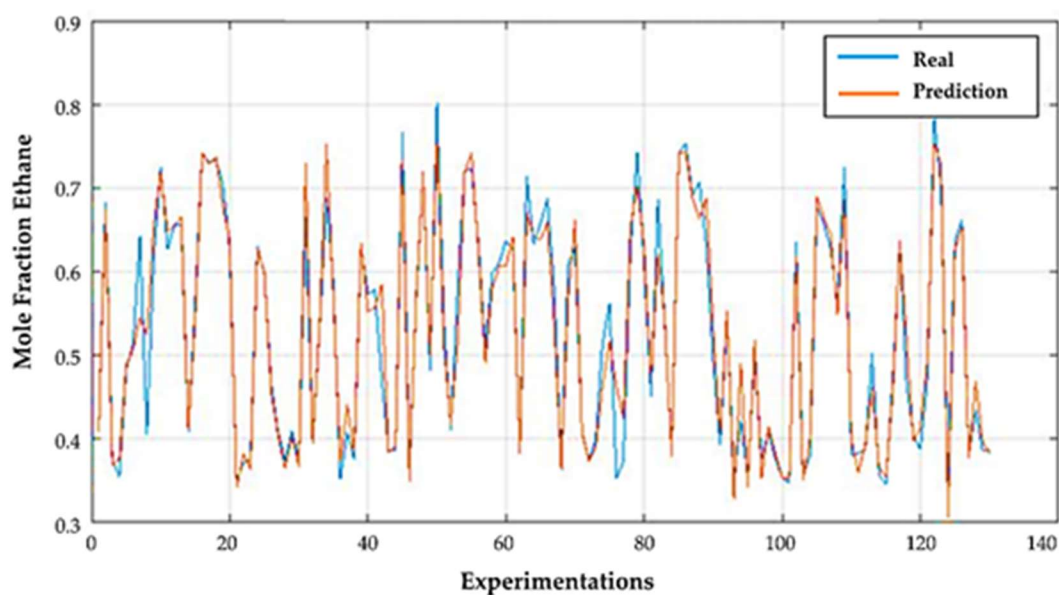


Figure 11. Comparison of DWSIM (real) and ANN (prediction) results on solvent recovery column bottoms (C3 mole fraction)

In this research we used the functions ANOVA and Kruskal-Wallis [52] using SPSS 22.0, to statistically validate the ANN. Table 11 shows the results from ANOVA and, for all cases, P-values (probability value in statistical significance tests) is greater than 0.05, while Table 12 summarizes the results of the Kruskal-Wallis test that was performed to validate of outliers of the predictions. This test also verifies that the P-value is greater than 0.05 in all cases, indicating that there is no statistically significant difference between the means of the observations and the predictions. These statistical tests reveal that the ANN constructed is statistically valid for the

prediction of the mole fractions of CO₂, C₂H₆ and C₃ in columns C1, C2 and C3, with a confidence level of 95%.

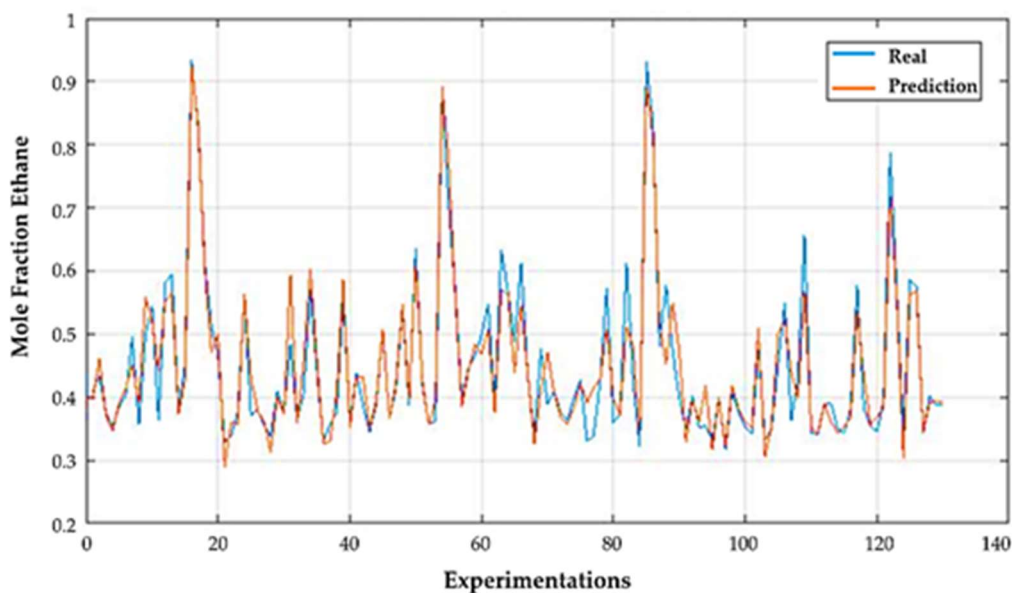


Figure 12. Comparison of DWSIM (real) and ANN (predicted) results in the concentrator column distillate (mole fraction of C₂H₆)

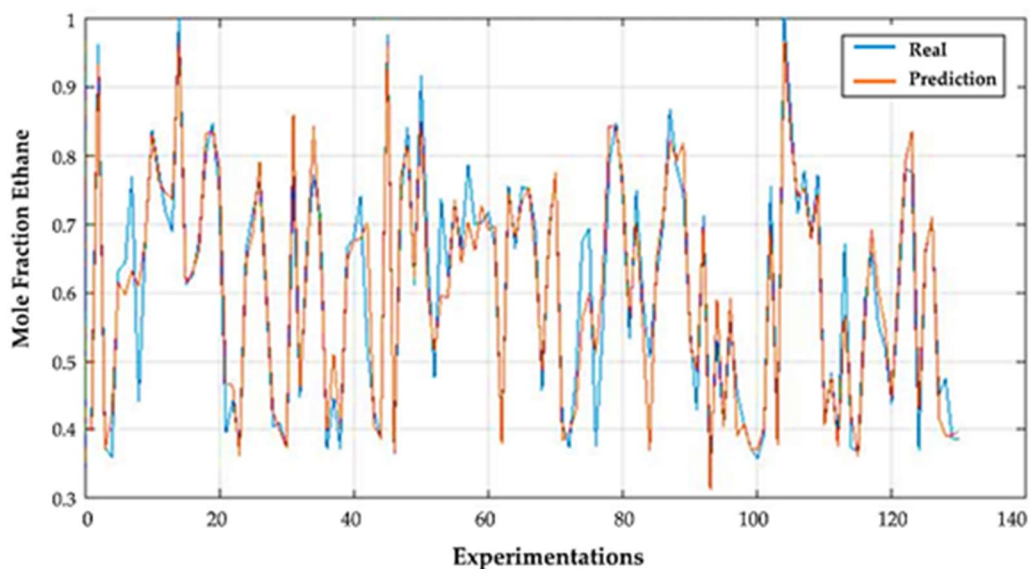


Figure 13. Comparison of DWSIM (real) and ANN (prediction) results on the concentrator column residue (mole fraction of C₂H₆)

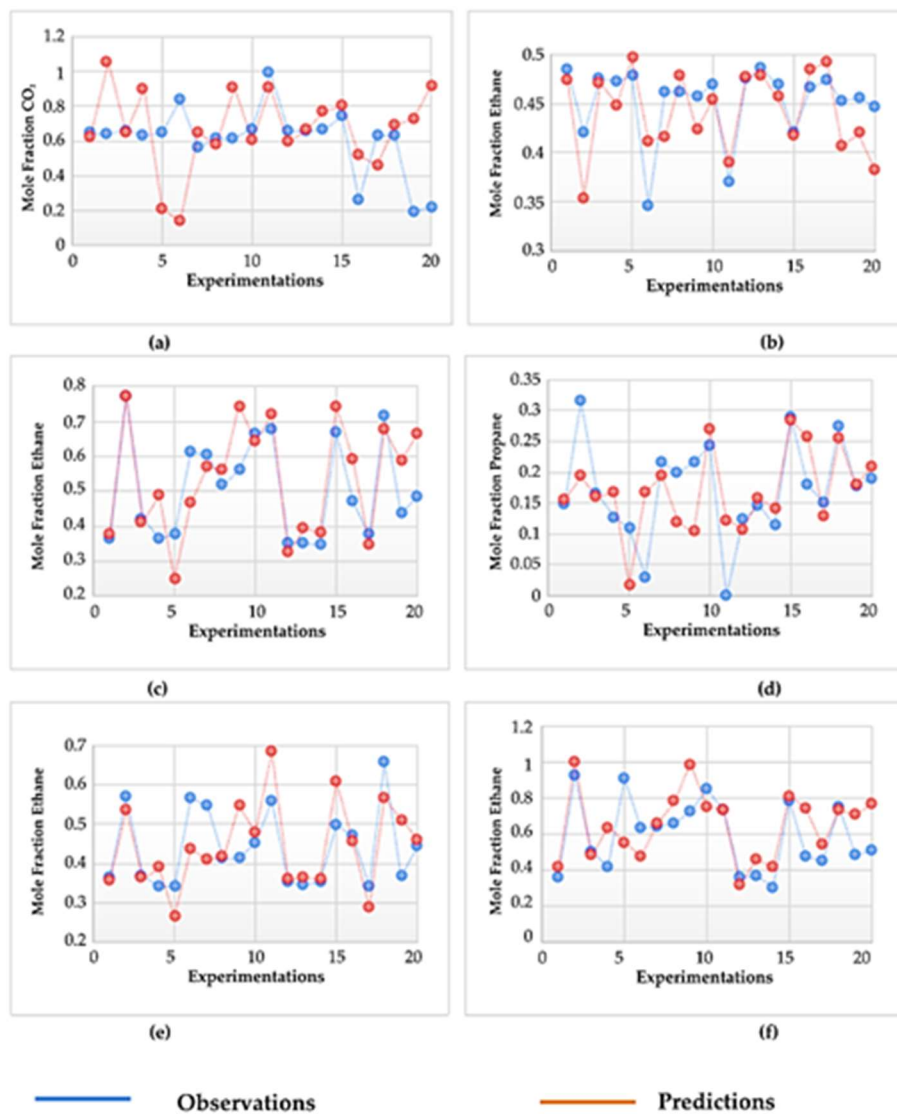


Figure 14. Comparison between observations and predictions. Extractive column: a) CO₂ mole fraction (distillate), b) C₂H₆ (bottoms); Solvent recovery column: c) C₂H₆ (distillate), d) C₃ (bot-toms); Concentrator column: e) C₂H₆ (distillate), f) C₂H₆ (bottoms).

Table 11. ANOVA

Source	Sum of squares	DOF	Mean square	F-Value	P-value
Mole fraction of CO₂ in the extractive column distillate					
Inter groups	0.0343	1	0.0343	0.78	0.383
Intra groups	1.6778	38	0.0441		
Total (Corr.)	1.7122	39			
Mole fraction of C₂H₆ in the extractive column bottoms.					
Inter groups	0.0010	1	0.0010	0.70	0.407
Intra groups	0.0572	38	0.0015		
Total (Corr.)	0.0583	39			

Mole fraction of C ₂ H ₆ in solvent recovery column distillate.					
Inter groups	0.0083	1	0.0083	0.37	0.549
Intra groups	0.8684	38	0.0228		
Total (Corr.)	0.8767	39			
Mole fraction of C ₃ in the solvent recovery column bottoms.					
Inter groups	2.38E-05	1	2.38E-05	0.00	0.946
Intra groups	0.1983	38	5.21E-03		
Total (Corr.)	0.1983	39			
Mole fraction of C ₂ H ₆ in the concentrator column distillate.					
Inter groups	1.79E-04	1	1.79E-04	0.02	0.897
Intra groups	0.4027	38	0.0105		
Total (Corr.)	0.4028	39			
Mole fraction of C ₂ H ₆ in the concentrator column bottoms.					
Inter groups	0.0321	1	0.0321	0.88	0.353
Intra groups	1.3843	38	0.0364		
Total (Corr.)	1.4164	39			

Table 12. Kruskal-Wallis Test

	Average Range	Statistical	P-value
Extractive column			
CO ₂ Observation (Distillate)	19.05	0.615	0.433
CO ₂ Prediction (Distillate)	21.95		
C ₂ H ₆ Observation (Bottoms)	21.75	0.457	0.499
C ₂ H ₆ Prediction (Bottoms)	19.25		
Solvent recovery column			
C ₂ H ₆ Observation (Bottoms)	19.25	0.457	0.499
C ₂ H ₆ Prediction (Bottoms)	21.75		
C ₃ Observation (Bottoms)	20.85	0.035	0.849
C ₃ Prediction (Bottoms)	20.15		
Concentrator column			
C ₂ H ₆ Observation (Bottoms)	19.95	0.088	0.767
C ₂ H ₆ Prediction (Bottoms)	21.05		
C ₂ H ₆ Observation (Bottoms)	18.75	0.896	0.344
C ₂ H ₆ Prediction (Bottoms)	22.25		

4. Conclusions

The mole fractions of an alternative extractive distillation system for the separation of CO₂-C₂H₆ azeotropes in enhanced oil recovery processes were predicted using an ANN based on the process simulation in DWSIM in this study. The ANN developed has 80 hidden neurons and was trained with a base of 130 pairs of data with 3 input variables (neurons): pressure (P), temperature (T), and solvent/feed ratio. It is capable of predicting 6 output variables (neurons): the mole fraction of CO₂ in the distillate and C₂H₆ in the bottoms of the extractive column (C1), the mole fraction

of C₂H₆ in the distillate and C₃ in the bottoms of the solvent recovery column (C₂), and the mole fractions of C₂H₆ in the distillate and in the bottoms of the concentrator column (C₃).

The Bayesian regularization approach was used to train the ANN, which has an MSE of 0.0036 and a total R of 0.95546. A comparison statistical analysis (ANOVA and Kruskal-Wallis) between the data (DWSIM) and the values predicted by the neural network was also used to validate the ANN. Statistical tests show that the ANN accurately predicts the mole fractions at the outputs with a 95% significance level.

According to the findings, the ANN developed in this work can be used as a prediction tool for improving natural gas sweetening operations. For instance, real operating parameters of the described process must be used as input, apply them in situ and verify the predictions at the control points (outputs of the ANN). Subsequently, validated in the plant and coupled to the existing control process, the energy optimization of the process can be promoted by coupling genetic optimization algorithms to the network (hybrid technologies). Optimization studies in a real plant will be the subject of future research.

Supplementary Materials: The following are available online at www.mdpi.com/xxx/s1, Figure S1: title, Table S1: title, Video S1: title.

Author Contributions: Conceptualization, D.C.H.V and W.D; methodology, W.D, and D.C.H.V ; software, W.D, N.C.H.V and J.C.H.V; ANN, N.C.H.V and J.C.H.V; validation, D.C.H.V and S.C; formal analysis, D.C.H.V and S.C; statistical analysis, N.C.H.V and J.C.H.V, data curation, D.C.H.V and S.C .; writing—original draft preparation, D.C.H.V and S.C; writing—review and editing, D.C.H.V and S.C; supervision, S.C; funding acquisition, N.C.H.V, J.C.H.V, D.C.H.V. All authors have read and agreed to the published version of the manuscript.

Acknowledgments: The author thanks the Security Research Group on Environment and Engineering, "GISAI" for allowing the execution of this research.

Conflicts of Interest: The authors declare no conflict of interest.

Appendix A

Database generated for simulation parameters, training and validation of the ANN

References

1. Lapuerta, A. El Gas Natural: Una posibilidad de combustible limpio en el Mercado Automotriz del Ecuador, Universidad Andina Simón Bolívar, 2008.
2. Perry, S.; Perry, R.H.; Green, D.W.; Maloney, J.O. Perry's chemical engineers' handbook; 2000; Vol. 38; ISBN 0070498415.
3. Gutiérrez, J.P.; Sosa, T.S.; Ale, R.; Zapata, A.R.; Erdmann, E. Diseño del Proceso de Endulzamiento de Gas Natural. Simulación y Comparación. In Proceedings of the VII Congreso Argentino de Ingeniería Química; 2013; p. 13.
4. Elliot, D.; Qualls, W.R.; Huang, S.; Chen, J.J.; Lee, R.J.; Yao, J.; Zhang, Y. Benefits of integrating NGL extraction and LNG liquefaction technology. In Proceedings of the AIChE 2005

Spring National Meeting 5th Topical Conference on Natural Gas Utilization (TI); Houston, 2005; pp. 1943–1958.

5. Ebrahimzadeh, E.; Matagi, J.; Fazlollahi, F.; Baxter, L.L. Alternative extractive distillation system for CO₂-ethane azeotrope separation in enhanced oil recovery processes. *Appl. Therm. Eng.* 2016, 96, 39–47, doi:10.1016/j.applthermaleng.2015.11.082.
6. Li, G.; Bai, P. New operation strategy for separation of ethanol-water by extractive distillation. *Ind. Eng. Chem. Res.* 2012, 51, 2723–2729, doi:10.1021/ie2026579.
7. Kiss, A.A.; Ignat, R.M. Enhanced methanol recovery and glycerol separation in biodiesel production - DWC makes it happen. *Appl. Energy* 2012, 99, 146–153, doi:10.1016/j.apenergy.2012.04.019.
8. Torres-Ortega, C.E.; Segovia-Hernández, J.G.; Gómez-Castro, F.I.; Hernández, S.; Bonilla-Petriciolet, A.; Rong, B.G.; Errico, M. Design, optimization and controllability of an alternative process based on extractive distillation for an ethane-carbon dioxide mixture. *Chem. Eng. Process. - Process Intensif.* 2013, 74, 55–68, doi:10.1016/j.cep.2013.09.011.
9. Lastari, F.; Pareek, V.; Trebble, M.; Tade, M.O.; Chinn, D.; Tsai, N.C.; Chan, K.I. Extractive distillation for CO₂-ethane azeotrope separation. *Chem. Eng. Process. Process Intensif.* 2012, 52, 155–161, doi:10.1016/j.cep.2011.10.001.
10. Tavan, Y.; Hosseini, S.H. A novel application of reactive absorption to break the CO₂-ethane azeotrope with low energy requirement. *Energy Convers. Manag.* 2013, 75, 407–417, doi:10.1016/j.enconman.2013.06.015.
11. Tavan, Y.; Shahhosseini, S.; Hosseini, S.H. Design and simulation of ethane recovery process in an extractive dividing wall column. *J. Clean. Prod.* 2014, 72, 222–229, doi:10.1016/j.jclepro.2014.03.015.
12. Tavan, Y.; Shahhosseini, S.; Hosseini, S.H. Feed-splitting technique in the extractive distillation of CO₂-ethane azeotropic process. *Sep. Purif. Technol.* 2014, 122, 47–53, doi:10.1016/j.seppur.2013.10.041.
13. Picaud-vannereux, S.; Lutin, F.; Favre, E.; Roizard, D. Energy efficiency of membrane vs hybrid membrane / cryogenic processes for propane recovery from nitrogen purging vents : A simulation study. *Sep. Purif. Technol.* 2020, 240, 116613, doi:10.1016/j.seppur.2020.116613.
14. Skiborowski, M.; Wessel, J.; Marquardt, W. Efficient optimization-based Design of Membrane-Assisted Distillation Processes. *Ind. Eng. Chem.* 2014, 20, doi:https://doi.org/10.1021/ie502482b.
15. Trubyanov, M.M.; Shablykin, D.N.; Mokhnachev, N.A.; Sergeeva, M.S.; Vorotyntsev, A. V.; Petukhov, A.N.; Vorotyntsev, V.M. Separation and Purification Technology A hybrid batch distillation / membrane process for high purification part 1 : Energy efficiency and separation performance study for light impurities removal. *Sep. Purif. Technol.* 2020, 241, 116678, doi:10.1016/j.seppur.2020.116678.
16. Khayet, M.; Cojocaru, C.; Essalhi, M. Artificial neural network modeling and response surface methodology of desalination by reverse osmosis. *J. Memb. Sci.* 2011, 368, 202–214, doi:10.1016/j.memsci.2010.11.030.

17. Khayet, M.; Cojocaru, C. Artificial neural network modeling and optimization of desalination by air gap membrane distillation. *Sep. Purif. Technol.* 2012, 86, 171–182, doi:10.1016/j.seppur.2011.11.001.
18. Montague, G.A.; Tham, M.T.; Willis, M.J.; Morris, A.J. Predictive Control of Distillation Columns Using Dynamic Neural Networks. *IFAC Proc. Vol.* 1992, 25, 243–248, doi:10.1016/s1474-6670(17)50999-4.
19. Zamprogna, E.; Barolo, M.; Seborg, D.E. Composition estimations in a middle-vessel batch distillation column using artificial neural networks. *Chem. Eng. Res. Des.* 2001, 79, 689–696, doi:10.1205/026387601316971361.
20. Ying, L.; Yao, W.; Yao, W.Y. Heat integration of the azeotropic distillation system with. In *Proceedings of the Proceedings of the 4th World Congress on Intelligent Control And Automation*; 2002; pp. 1573–1577.
21. Liao, L.C.; Yang, T.C.; Tsai, M. Expert system of a crude oil distillation unit for process optimization using neural networks. *Expert Syst. Appl.* 2004, 26, 247–255, doi:10.1016/S0957-4174(03)00139-8.
22. Fernandez de Canete, J.; Gonzalez-Perez, S.; Saz-Orozco, P. Artificial Neural Networks for Identification and Control of a Lab-Scale Distillation Column using LABVIEW. *Eng. Technol.* 2008, 2, 64–69, doi:10.5281/zenodo.1056278.
23. Motlaghi, S.; Jalali, F.; Ahmadabadi, M.N. An expert system design for a crude oil distillation column with the neural networks model and the process optimization using genetic algorithm framework. *Expert Syst. Appl.* 2008, 35, 1540–1545, doi:10.1016/j.eswa.2007.08.105.
24. Vafaei, M.T.; Eslamloueyan, R.; Ayatollahi, S. Simulation of steam distillation process using neural networks. *Chem. Eng. Res. Des.* 2009, 87, 997–1002, doi:10.1016/j.cherd.2009.02.006.
25. Ochoa-Estopier, L.M.; Jobson, M.; Smith, R. Operational optimization of crude oil distillation systems using artificial neural networks. *Comput. Chem. Eng.* 2013, doi:10.1016/j.compchemeng.2013.05.030.
26. Leng, W.; Zhan, H.; Ge, L.; Wang, W.; Ma, Y.; Zhao, K.; Li, S.; Xiao, L. Rapidly determining the principal components of natural gas distilled from shale with terahertz spectroscopy. *Fuel* 2015, 159, 84–88, doi:10.1016/j.fuel.2015.06.072.
27. Osulale, F.N.; Zhang, J. Energy efficiency optimisation for distillation column using artificial neural network models. *Energy* 2016, 106, 562–578, doi:10.1016/j.energy.2016.03.051.
28. Ye, R.P.; Ding, J.; Gong, W.; Argyle, M.D.; Zhong, Q.; Wang, Y.; Russell, C.K.; Xu, Z.; Russell, A.G.; Li, Q.; et al. CO₂ hydrogenation to high-value products via heterogeneous catalysis. *Nat. Commun.* 2019, 10.
29. Sánchez-Escalona, A.A.; Góngora-Leyva, E.; Zalazar-Oliva, C. Predicción de la resistencia térmica de las incrustaciones en los enfriadores de ácido sulfhídrico. *Minería y Geol.* 2018, 34, 90–100.
30. Kamble, L. V.; Pangavhane, D.R.; Singh, T.P. Heat transfer studies using artificial neural network - A review. *Int. Energy J.* 2014, 14, 25–42.

31. Mohanraj, M.; Jayaraj, S.; Muraleedharan, C. Applications of artificial neural networks for thermal analysis of heat ex-changers - A review. *Int. J. Therm. Sci.* 2015, 90, 150–172, doi:10.1016/j.ijthermalsci.2014.11.030.
32. DWSIM DWSIM – The Open Source Chemical Process Simulator – Just another WordPress site 2020.
33. Dimian, A.C.; Bildea, C.S.; Kiss, A.A. Introduction in Process Simulation. In *Integrated Design and Simulation of Chemical Processes*; Elsevier: Amsterdam, 2014; Vol. 35, pp. 35–71 ISBN 9780444627001.
34. Kiss, A.A. *Advanced distillation technologies - Design, Control and Applications*; Wiley, J., Ed.; First.; Wiley: Noida, India., 2013; ISBN 9781119993612.
35. Soave, G.; Gamba, S.; Pellegrini, L.A. SRK equation of state: Predicting binary interaction parameters of hydrocarbons and related compounds. *Fluid Phase Equilib.* 2010, 299, 285–293, doi:10.1016/j.fluid.2010.09.012.
36. Tavan, Y. A note on use of the CO₂-ethane azeotrope as new feed of reforming process using mathematical modeling. *J. Nat. Gas Sci. Eng.* 2014, 21, 275–282, doi:10.1016/j.jngse.2014.08.004.
37. Lastari, F. *Ryan-Holmes and Modified Ryan-Holmes Processes for LNG Production*, Curtin University of Technology, 2009.
38. ZareNezhad, B.; Hosseinpour, N. An extractive distillation technique for producing CO₂ enriched injection gas in enhanced oil recovery (EOR) fields. *Energy Convers. Manag.* 2009, 50, 1491–1496, doi:10.1016/j.enconman.2009.02.016.
39. Chen, Y.; Song, L.; Liu, Y.; Yang, L.; Li, D. A review of the artificial neural network models for water quality prediction. *Appl. Sci.* 2020, 10, doi:10.3390/app10175776.
40. Chuquin-Vasco, D.; Parra, F.; Chuquin-Vasco, N.; Chuquin-Vasco, J.; Lo-Iacono-, V. Prediction of methanol production in a carbon dioxide hydro- genation plant using neural networks . *Energies* 2021, 14, 1–18, doi:10.3390/en14133965.
41. Singh, V.; Gupta, I.; Gupta, H.O. ANN based estimator for distillation - Inferential control. *Chem. Eng. Process. Process Intensif.* 2005, 44, 785–795, doi:10.1016/j.cep.2004.08.010.
42. Pedregosa, F.; Varauaux, G.; Gramfort, A.; Vincent, M.; Thirion, B. *Scikit-learn: Machine Learning in Python* Fabian, 2011, Vol. 12.
43. Bloice, M.D.; Holzinger, A. *A tutorial on machine learning and data science tools with python*; 2016; Vol. 9605 LNCS; ISBN 9783319504780.
44. Kayri, M. Predictive abilities of Bayesian regularization and levenberg-marquardt algorithms in artificial neural networks: A comparative empirical study on social data. *Math. Comput. Appl.* 2016, 21, doi:10.3390/mca21020020.
45. Bharati, S.; Rahman, M.; Podder, P.; Robel, M.R.; Gandhi, N. Comparative Performance Analysis of Neural Network Base Training Algorithm and Neuro-Fuzzy System with SOM for the Purpose of Prediction of the Features of Superconductors Subrato; 2019; Vol. 1181; ISBN 9783030295127.

46. Saini, L.M. Peak load forecasting using Bayesian regularization, Resilient and adaptive backpropagation learning based artificial neural networks. *Electr. Power Syst. Res.* 2008, 78, 1302–1310, doi:10.1016/j.epsr.2007.11.003.
47. Wang, L.; Wu, B.; Zhu, Q.; Zeng, Y.R. Forecasting Monthly Tourism Demand Using Enhanced Backpropagation Neural Network. *Neural Process. Lett.* 2020, 52, 2607–2636, doi:10.1007/s11063-020-10363-z.
48. Zeng, Y.R.; Zeng, Y.; Choi, B.; Wang, L. Multifactor-influenced energy consumption forecasting using enhanced back-propagation neural network. *Energy* 2017, 127, 381–396, doi:10.1016/j.energy.2017.03.094.
49. Suliman, A.; Omarov, B. Applying Bayesian Regularization for Acceleration of Levenberg Marquardt based Neural Net-work Training. *Int. J. Interact. Multimed. Artif. Intell.* 2018, 5, 68, doi:10.9781/ijimai.2018.04.004.
50. Garoosiha, H.; Ahmadi, J.; Bayat, H. The assessment of Levenberg–Marquardt and Bayesian Framework training algo-rithm for prediction of concrete shrinkage by the artificial neural network. *Cogent Eng.* 2019, 6, doi:10.1080/23311916.2019.1609179.
51. Abiodun, O.I.; Jantan, A.; Omolara, A.E.; Dada, K.V.; Mohamed, N.A.E.; Arshad, H. State-of-the-art in artificial neural network applications: A survey. *Heliyon* 2018, 4, e00938, doi:10.1016/j.heliyon.2018.e00938.
52. Kyono, K.; Hashimoto, T.; Nagai, Y.; Sakuraba, Y. Analysis of endometrial microbiota by 16S ribosomal RNA gene se-quencing among infertile patients: a single-center pilot study. *Reprod. Med. Biol.* 2018, 17, 297–306, doi:10.1002/rmb2.12105.